HUNTING SIGNALS OF DARK MATER IN CURRENT AND FUTURE COLLIDERS

Jaime Hernández-Sánchez
(Benemérita Universidad Autónoma de Puebla)

In collaboration with: A. Day, V. Keus, C. G. Honorato, S. King, S. Moretti, T. Sindou

OUTLINE

- Considering some models of 3HDM (in version I(2+1)HDM) symmetric under Z_2, $Z_2 \times Z_2'$ and Z_3, we analyze interesting signals of DM that could be tested in the colliders: LHC, ILC and LHeC.
- Assuming that the parameter space is constrained by EWPT, DM relic density limit, DD and ID searches for DM particles. These constraints provide DM candidate(s). (See the talk of Stefano Moretti)
- In the I(2+1)HDM symmetric under Z_2, we study for LHC case, the cascade decay of the SM-like Higgs boson (h):
  - $h \to H_1 H_2 \to H_1 H_1 f\bar{f}$ as a smoking-gun signal of 3HDM, where $H_2 \to H_1 \gamma^* \to H_1 f\bar{f}$ is induced at one-loop level.
- In the I(2+1)HDM symmetric under $Z_2 \times Z_2'$ (with two DM candidates): we study $e^+e^- \to DMDM\ell^+\ell^-$ (for ILC machine) in two cases:
  - The two DM candidates have the same CP (H_1, H_2) and opposite CP in another (H_1, A_2)
  - The distributions of observables for this collider can distinguish clearly both cases
- Prospects:
- Special case of I(2+1)HDM symmetric under Z_3 (we called hermaphrodite DM scenario), where one can has two DM candidates (H_1, A_1) and for ILC machine could be tested and distinguished with latter case $Z_2 \times Z_2'$.
- Signals in electron-proton colliders like LHeC, FCC-he: $e^-p \to DMDMj\ell^-$ or $e^-p \to DMDMj\nu$ or considering cascades of heavier scalar inserts having the final signatures: $\not{E}_T\, j$, $\not{E}_T \ell j$, $\not{E}_T 2\ell j$, $\not{E}_T 3\ell j$

I(2+1)HDM symmetric under Z_2,

- 3HDM is symmetric under Z_2 considering the generator $g_{Z_2} = diag(-1, -1, +1)$
- The potential symmetric under this symmetry is:
  - $$\begin{aligned} V &= V_0 + V_{Z_2}, \\ V_0 &= -\mu_1^2(\phi_1^\dagger\phi_1) - \mu_2^2(\phi_2^\dagger\phi_2) - \mu_3^2(\phi_3^\dagger\phi_3) \\ &+\lambda_{11}(\phi_1^\dagger\phi_1)^2 + \lambda_{22}(\phi_2^\dagger\phi_2)^2 + \lambda_{33}(\phi_3^\dagger\phi_3)^2 \\ &+\lambda_{12}(\phi_1^\dagger\phi_1)(\phi_2^\dagger\phi_2) + \lambda_{23}(\phi_2^\dagger\phi_2)(\phi_3^\dagger\phi_3) + \lambda_{31}(\phi_3^\dagger\phi_3)(\phi_1^\dagger\phi_1) \\ &+\lambda'_{12}(\phi_1^\dagger\phi_2)(\phi_2^\dagger\phi_1) + \lambda'_{23}(\phi_2^\dagger\phi_3)(\phi_3^\dagger\phi_2) + \lambda'_{31}(\phi_3^\dagger\phi_1)(\phi_1^\dagger\phi_3), \\ V_{Z_2} &= -\mu_{12}^2(\phi_1^\dagger\phi_2) + \lambda_1(\phi_1^\dagger\phi_2)^2 + \lambda_2(\phi_2^\dagger\phi_3)^2 + \lambda_3(\phi_3^\dagger\phi_1)^2 + \text{h.c.} \end{aligned}$$
- The minimum of the potential is given the following way ($m_h^2 = 2\mu_3^2$):
- $$\phi_1 = \begin{pmatrix} \phi_1^+ \\ \frac{H_1^0 + iA_1^0}{\sqrt{2}} \end{pmatrix}, \quad \phi_2 = \begin{pmatrix} \phi_2^+ \\ \frac{H_2^0 + iA_2^0}{\sqrt{2}} \end{pmatrix}, \quad \phi_3 = \begin{pmatrix} G^+ \\ \frac{v + h + iG^0}{\sqrt{2}} \end{pmatrix},$$
- We simplify the model and use the dark democracy limit (n=1):
- $$\mu_1^2 = n\mu_2^2, \quad \lambda_3 = n\lambda_2, \quad \lambda_{31} = n\lambda_{23}, \quad \lambda'_{31} = n\lambda'_{23},$$

THEORETICAL AND EXPERIMENTAL CONSTRAINTS
(SEE THE TALK OF STEFANO MORETTI)

- EW precision Test (EWPT)
- Collider data LEP and LHC: Higgs total decay width, Higgs invisible decays, on-shell decays from Z, W.
- The DM relic density.
- DD and ID detection.
- Being H_1 the DM candidate with two possibilities:
    - H_1 provides 100 % of DM (e.g. $m_{H_2} - m_{H_1} = 50$ GeV)
    - H_1 has subdominant contribution and (e.g. when $m_{H_2} - m_{H_1} = 5{,}10$ GeV).
    - The all heavier inert particles decay inside the detector(in particular H_2)

The cascade decay of SM-like Higgs boson h

- The Higgs boson h is produced by ggF or VBF in LHC
- $h \to H_1 H_2 \to H_1 H_1 f\bar{f}$ as a smoking-gun signal of 3HDM,
- $H_2 \to H_1 \gamma^* \to H_1 f\bar{f}$ is induced at one-loop level.

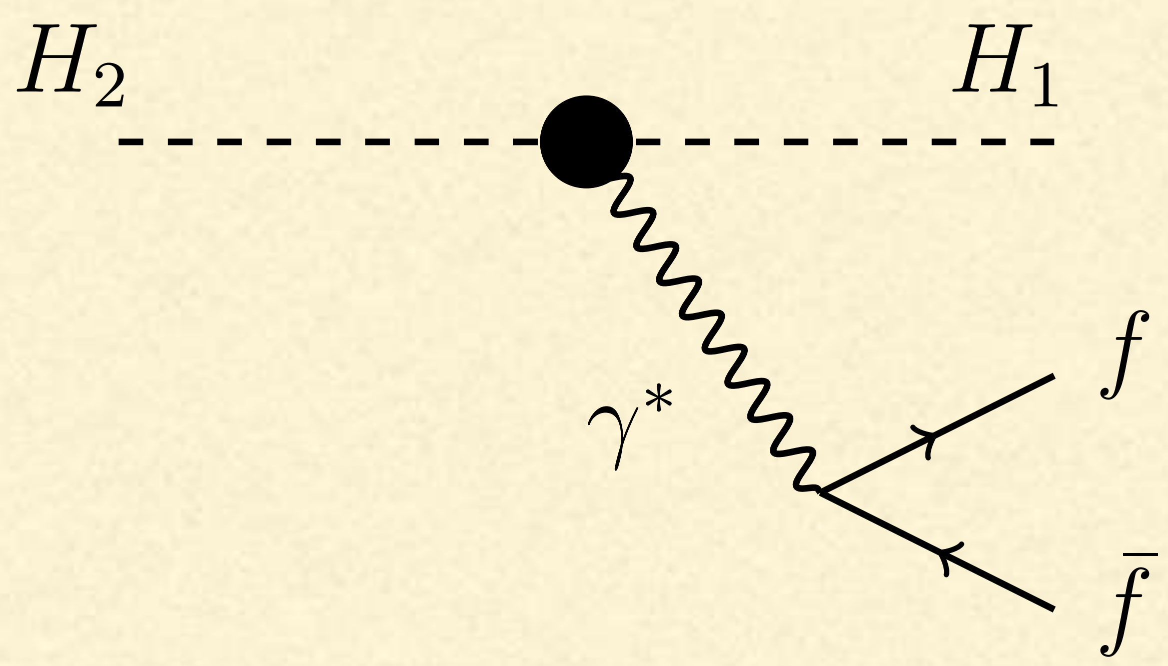

Is possible in the I(2+1)HDM and does not appear in I(1+1)HDM (H_1, A_1)

This a smoking-gun signal of the I(2+1)HDM

If $m_{f\bar{f}} < < m_Z$ then can potentially be extracted already from combining Run 2 and 3 data.

ArXiv: 1712.09598 [hep-ph]

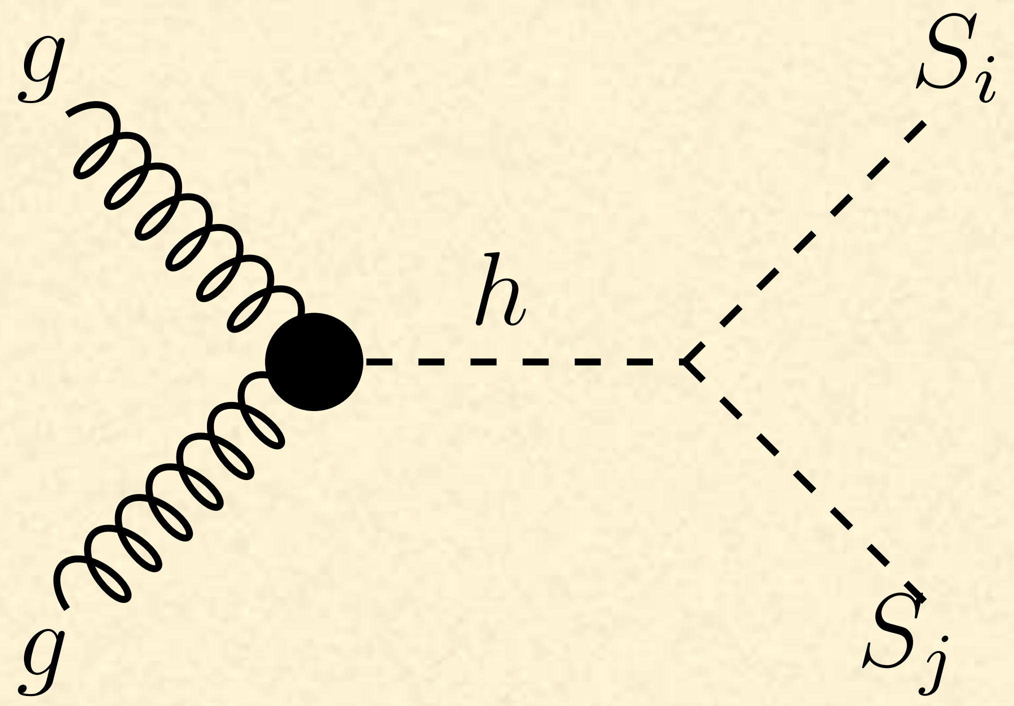

ggF

$$gg \to h \to H_1H_2 \to H_1H_1\gamma^* \to H_1H_1\ell\bar{\ell},$$

$$gg \to h \to H_2H_2 \to H_1H_1\gamma^*\gamma^* \to H_1H_12\ell2\bar{\ell}.$$

Higgs production and loop decay resonant

$$gg \to h \to H_i^{\pm}H_i^{\mp} \to H_1H_1W^{+(*)}W^{-(*)} \to H_1H_1\nu_l\ell\nu_l\bar{\ell} \quad (i=1,2),$$

$$gg \to h \to A_iA_j \to H_1H_1Z^{(*)}Z^{(*)} \to H_1H_12\ell2\bar{\ell} \quad (i=1,2),$$

Subdominant processes by restrictions of parameter space

However, there is an alternative method to generate the final state $H_1H_1f\bar{f}$

This process also emerges from s-channel quark-antiquark annihilation, producing a virtual neutral massive gauge boson. More explicitly:

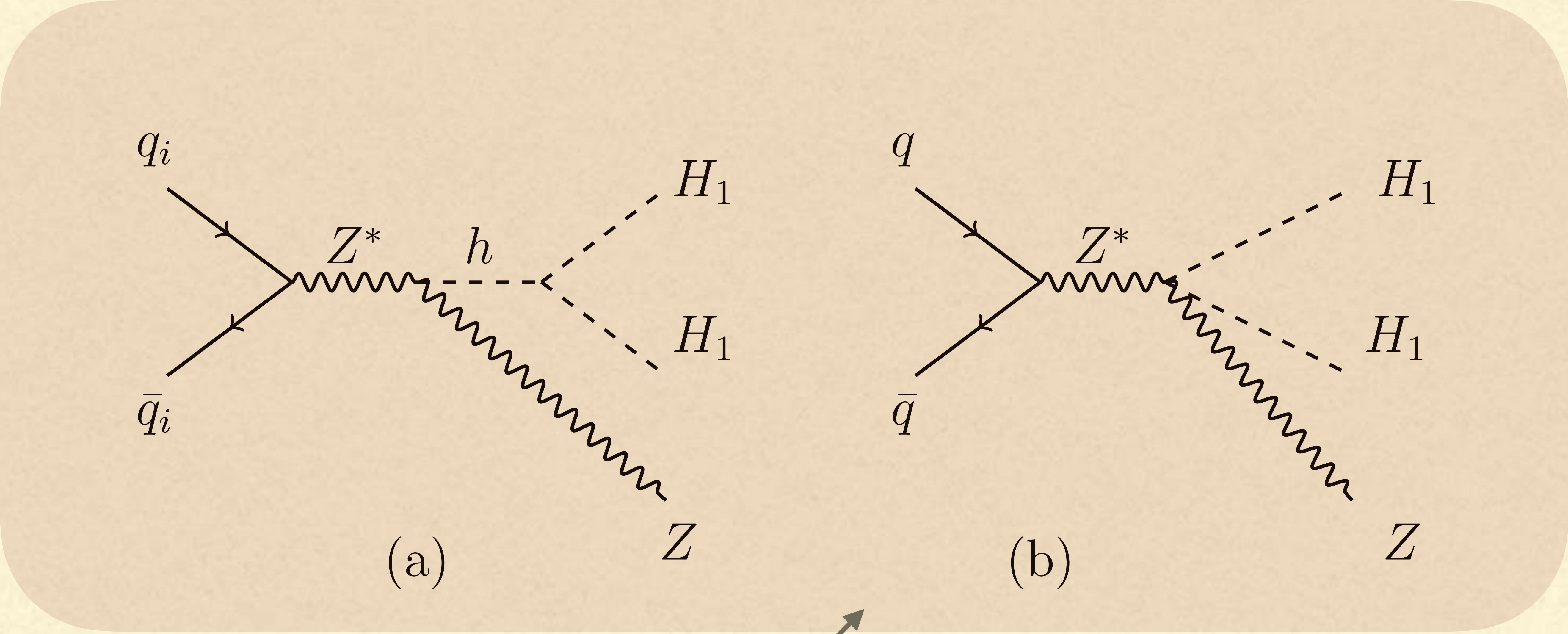

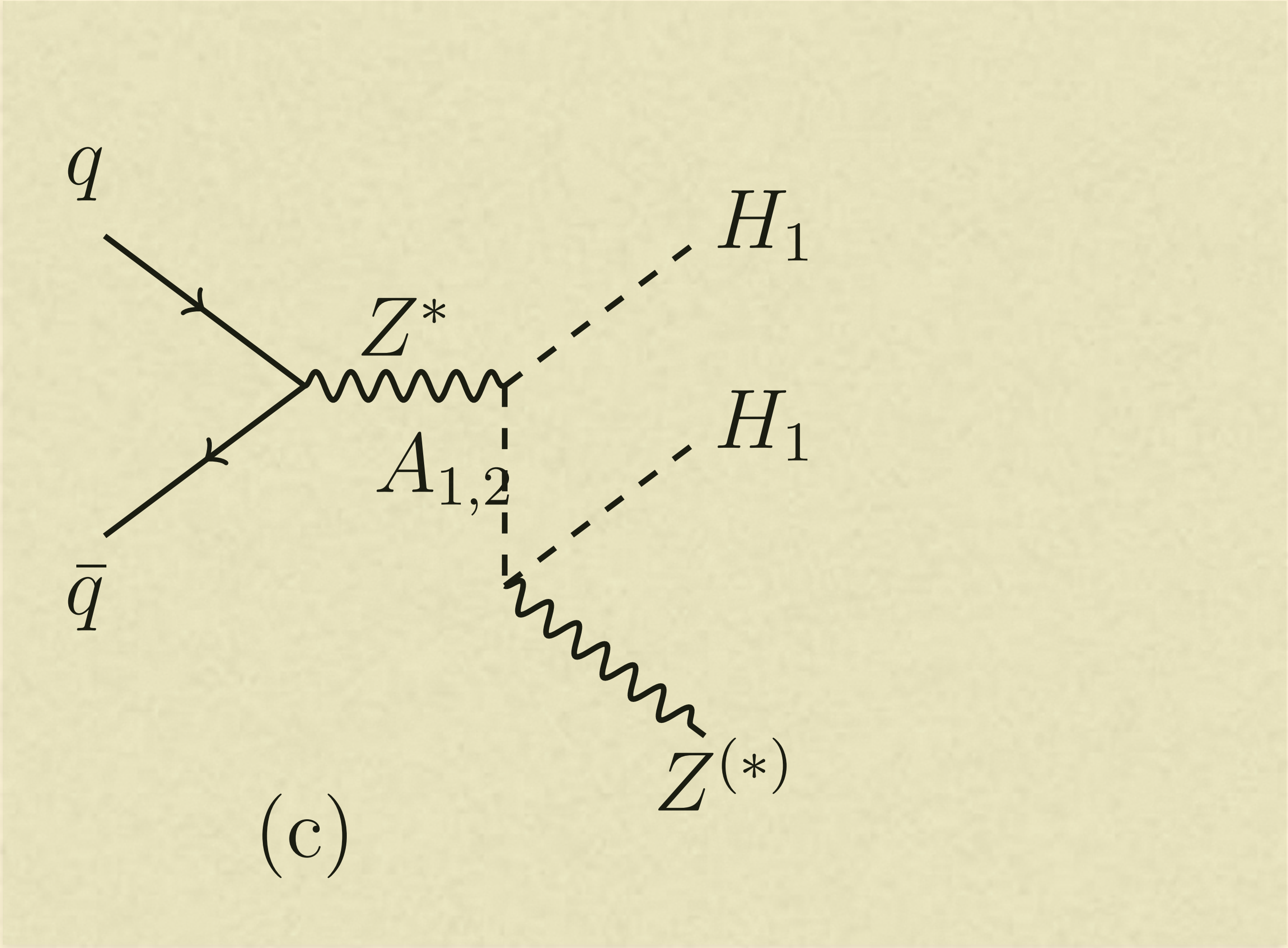

Is competitive with:

$$gg \to h \to H_1H_2 \to H_1H_1\gamma^* \to H_1H_1\ell\bar{\ell},$$

Constrained by $g_{H_1H_1h}$ and parameter space

But negligibly for the signal for $\not{E}_T 2\ell 2\ell$

VBF

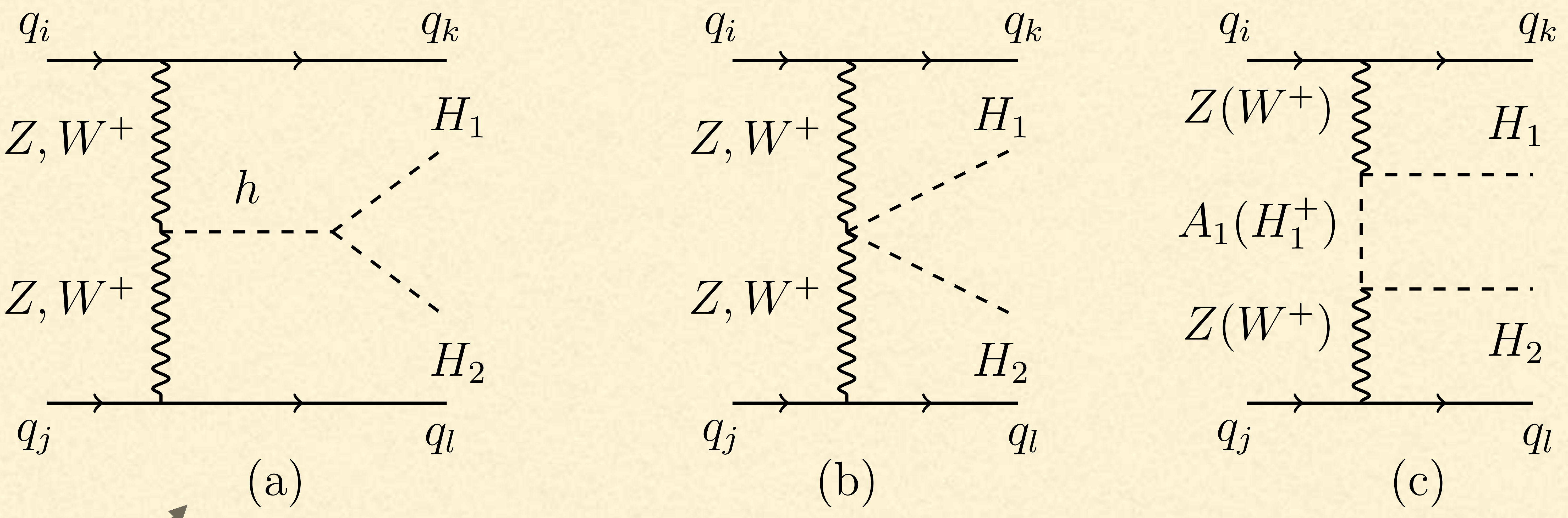

When Higgs boson can resonate, is dominant

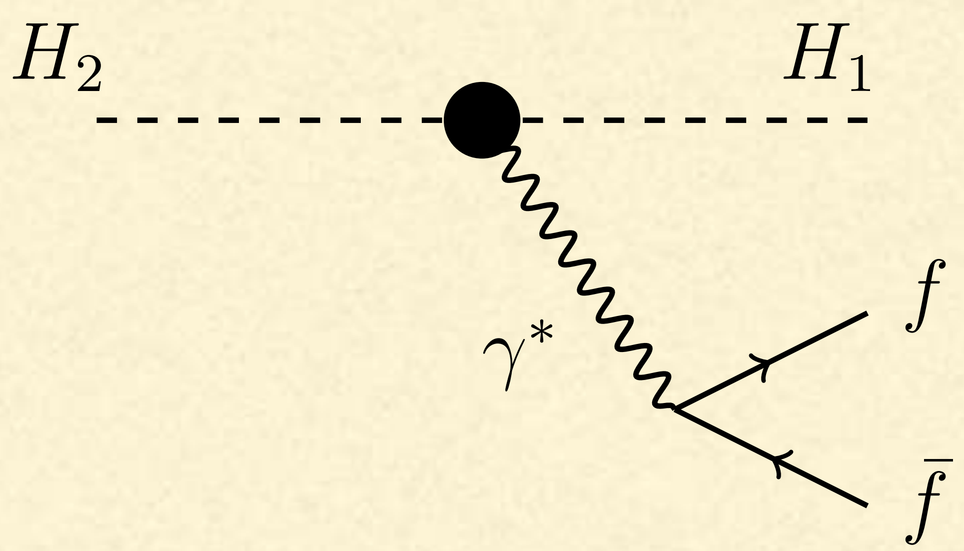

The loop calculation $H_2 \to H_1\gamma^* \to H_1 f\bar{f}$

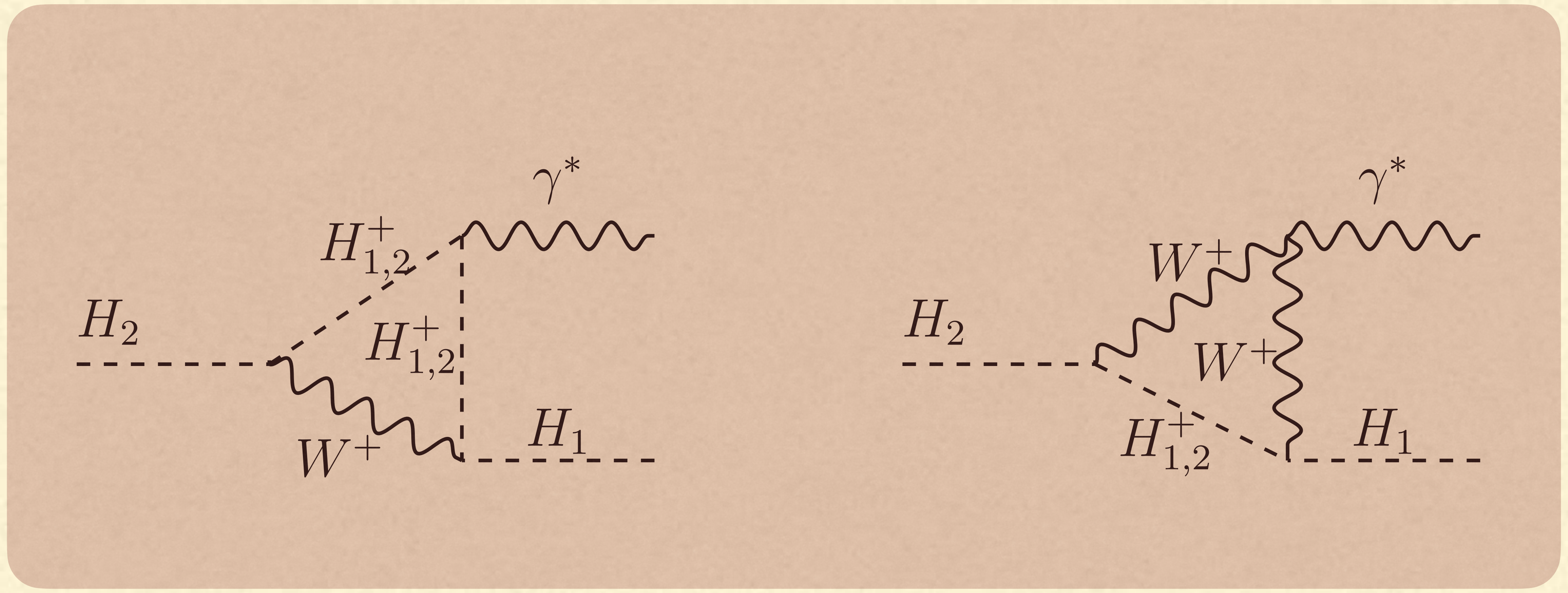

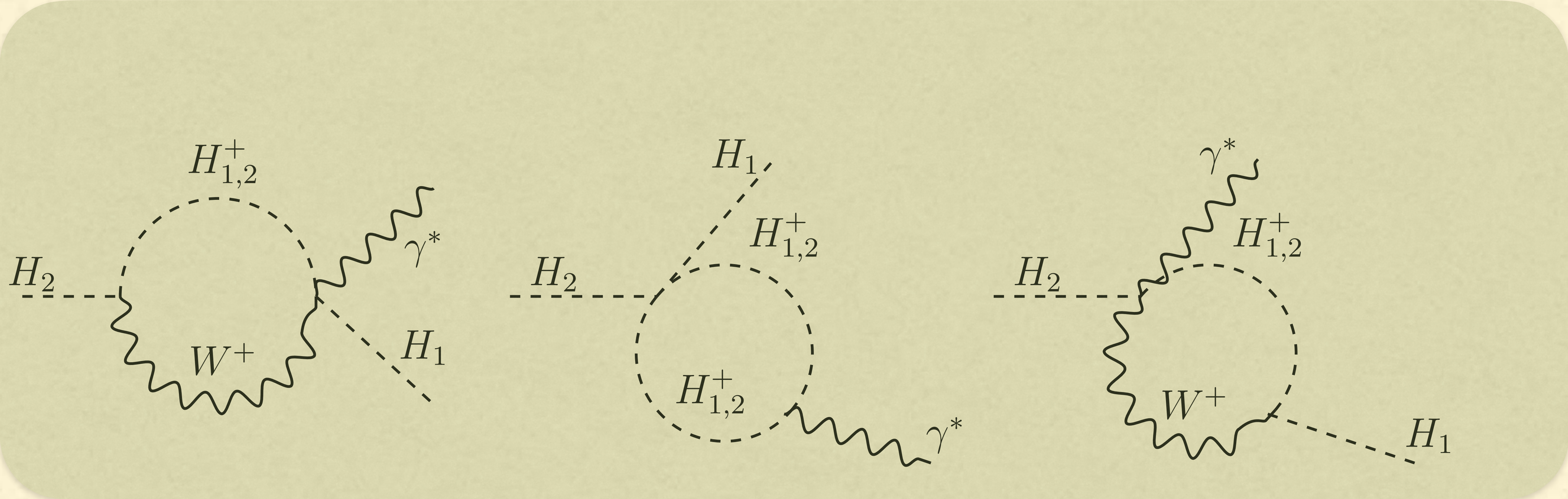

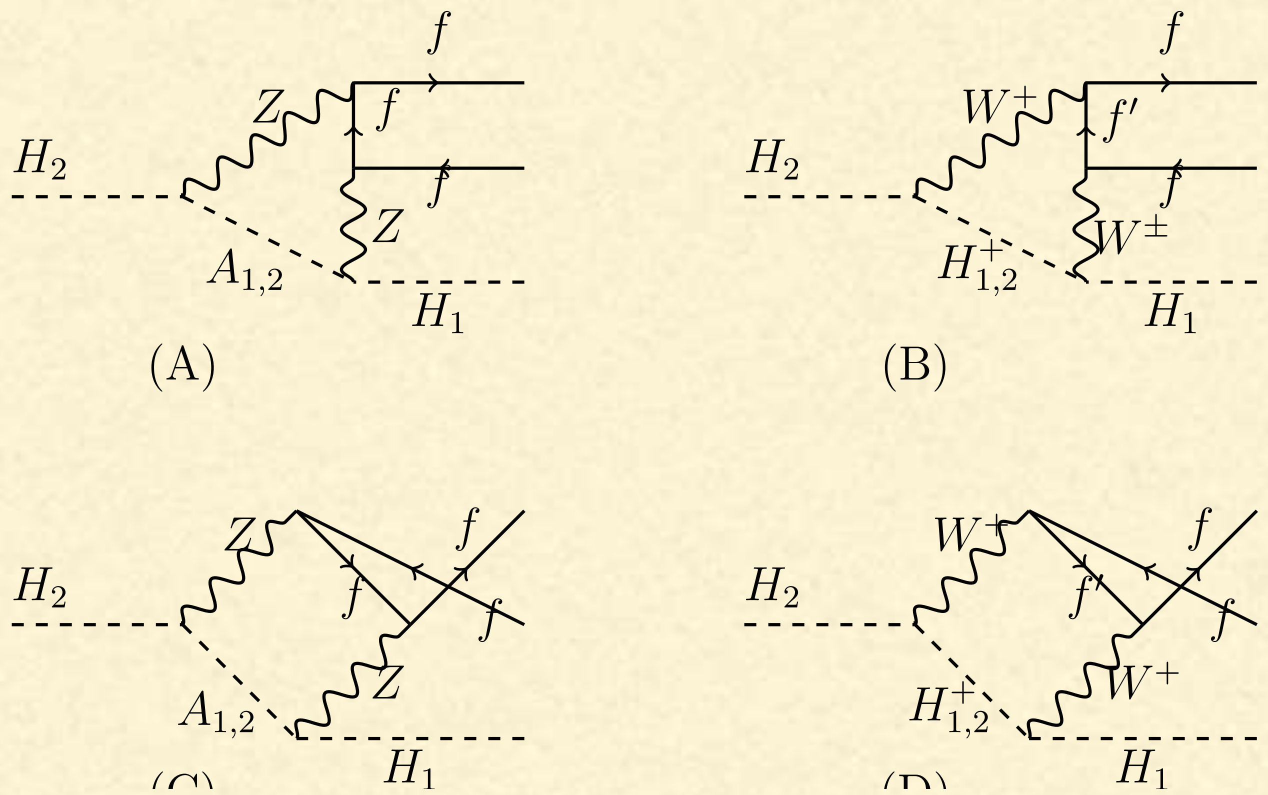

The general estructure of the cascade decay of H_2 is:

$$\mathcal{M} = ie\bar{v}(k_1)\gamma^\nu u(k_2)\frac{ig_{\mu\nu}}{(p_3-p_2)^2}[A(p_3+p_2)^\mu],$$

$$A(p_3+p_2)^\mu = M_{\mu,T} = \sum_i M_\mu^{(i)},$$

$$M_{\mu,T}(m_{H_i^\pm}, m_W, m_{12}^2, m_{H_i}) = eg^2\sum_{i=1}^{2}\sum_{k=1}^{4}(A_i^+ + A_i^-)m_\mu^{(k)}(m_{H_i^\pm}, m_W, m_{12}^2, m_{H_i}).$$

$$\begin{aligned}
A^+_{H_1^+,H_2} &= \cos(\theta_c-\theta_h)\sin(\theta_c-\theta_h),\\
A^+_{H_1^+,A_1} &= \cos(\theta_a-\theta_c)\cos(\theta_c-\theta_h),\\
A^+_{H_1^+,A_2} &= \sin(\theta_c-\theta_a)\cos(\theta_c-\theta_h),\\
A^+_{H_2^+,A_1} &= \sin(\theta_a-\theta_c)\sin(\theta_c-\theta_h),\\
A^+_{H_2^+,A_2} &= \cos(\theta_a-\theta_c)\sin(\theta_c-\theta_h),
\end{aligned}$$

$$\begin{aligned}
A_1^- &= A_1^{+*} = A_1^+,\\
A_2^+ &= -A_1^+\\
A_2^- &= -A_1^{+*} = -A_1^-.
\end{aligned}$$

$$M_{\mu,T}(m_{H_i^\pm}, m_W, m_{12}^2, m_{H_i}) = eg^2 A_1^\pm\sum_{k=1}^{4}\delta m_\mu^{(k)}(m_{H_1^\pm}, m_{H_1^\pm})$$

$$\delta m_\mu^{(k)}(m_{H_1^\pm}, m_{H_1^\pm}) = \left(m_\mu^{(k)}(m_{H_1^\pm}, m_W, m_{12}^2, m_{H_i}) - m_\mu^{(k)}(m_{H_2^\pm}, m_W, m_{12}^2, m_{H_i})\right).$$

The ultraviolet divergencies are cancelled perfectly!

Benchmark	$m_{H_2} - m_{H_1}$	$m_{A_1} - m_{H_1}$	$m_{A_2} - m_{H_1}$	$m_{H_1^\pm} - m_{H_1}$	$m_{H_2^\pm} - m_{H_1}$
A50	50	75	125	75	125
I5	5	10	15	90	95
I10	10	20	30	90	100

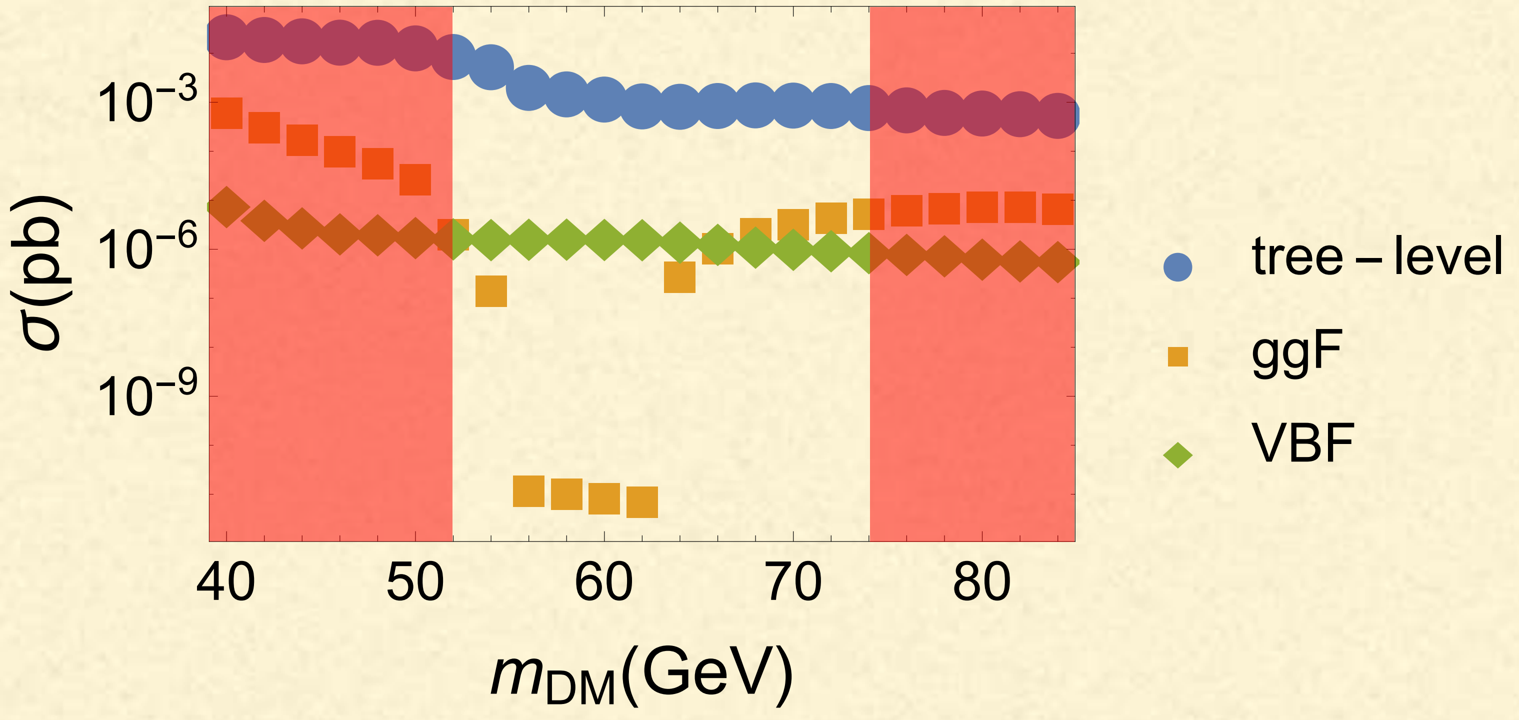

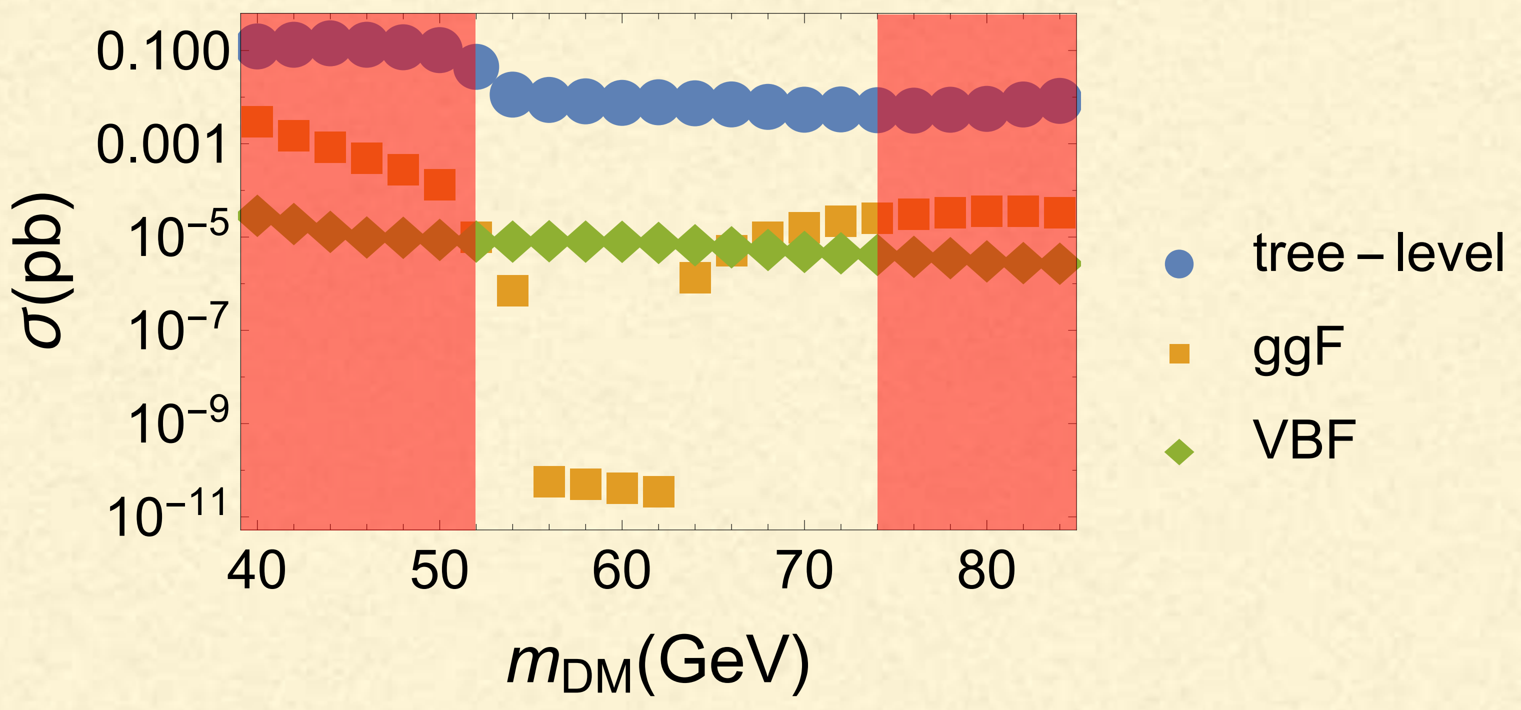

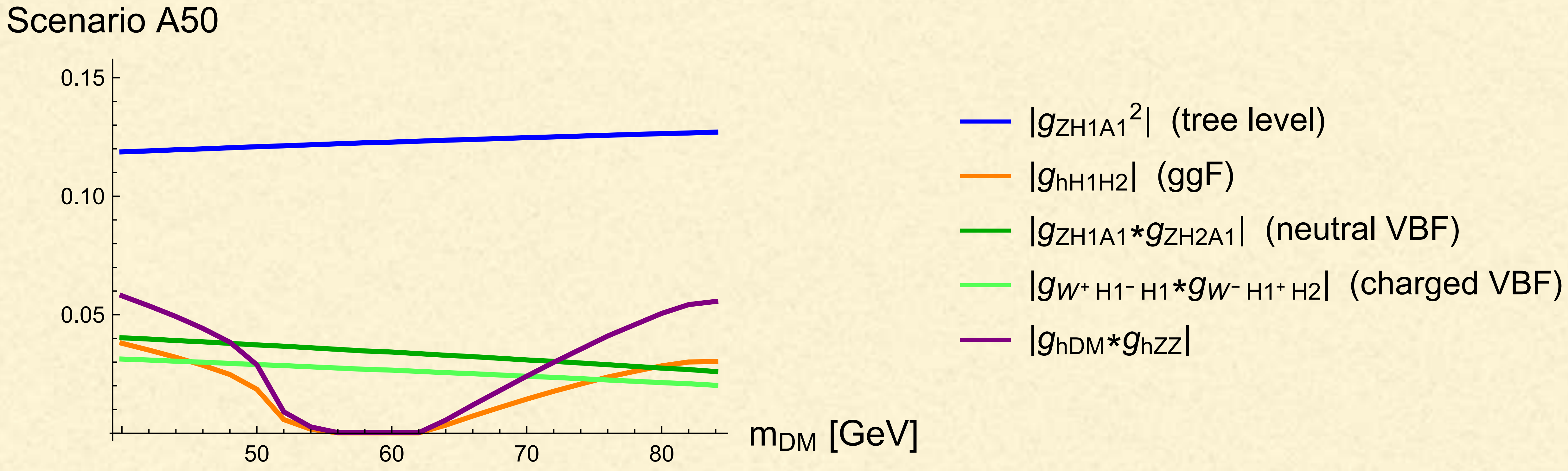

Scenario A50. The red regions are ruled out by LHC ($m_{DM} < 53$ GeV) and by direct detection ($m_{DM} > 73$ GeV). At the bottom we show the dominant couplings in each process with the same color coding where the Higgs-DM coupling is shown for reference.

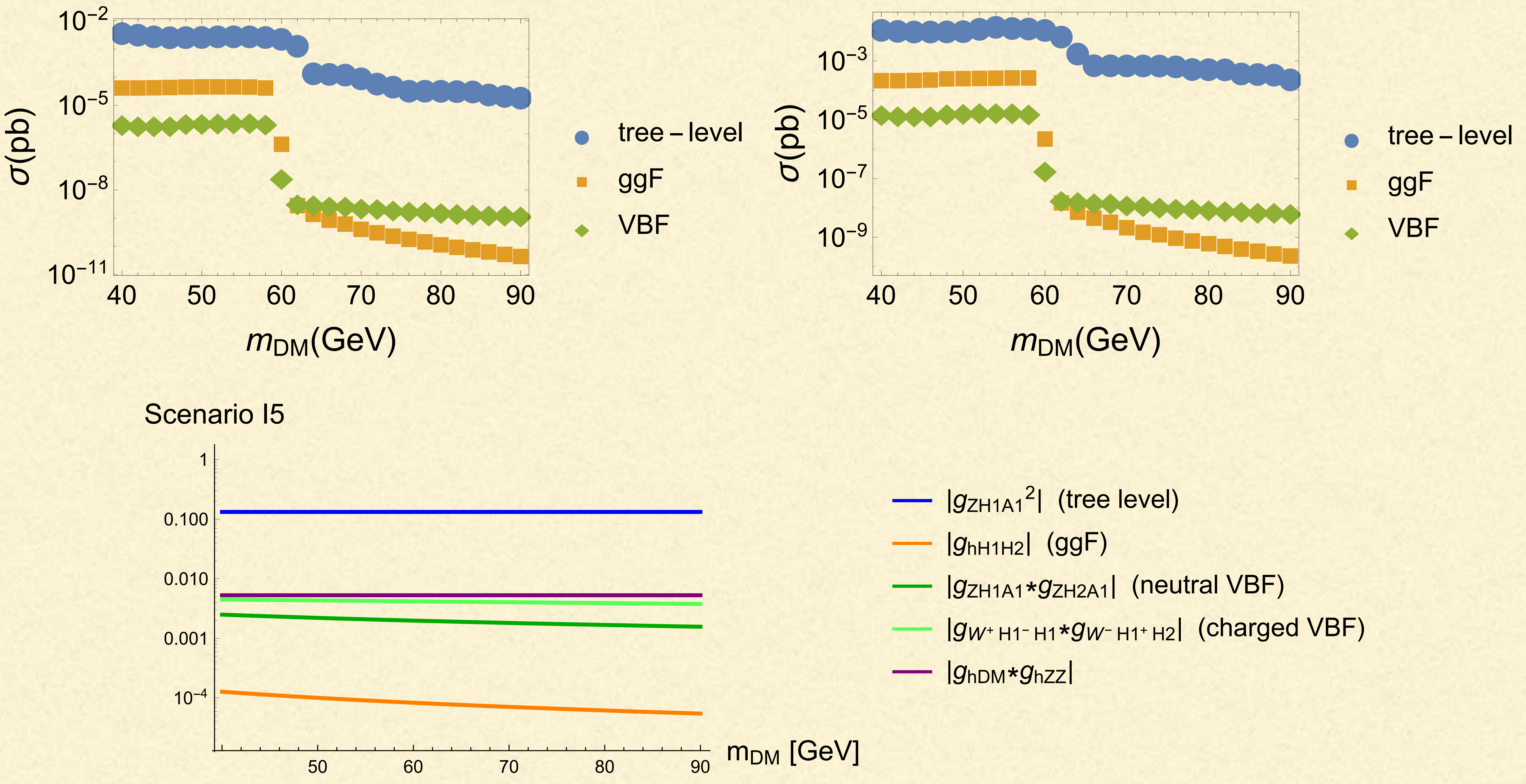

Scenario I5. The plots on the top show the cross sections of the tree-level, ggF and VBF processes with leptonic (left) and hadronic (right) final states. At the bottom we show the dominant couplings, where the Higgs-DM coupling is shown.

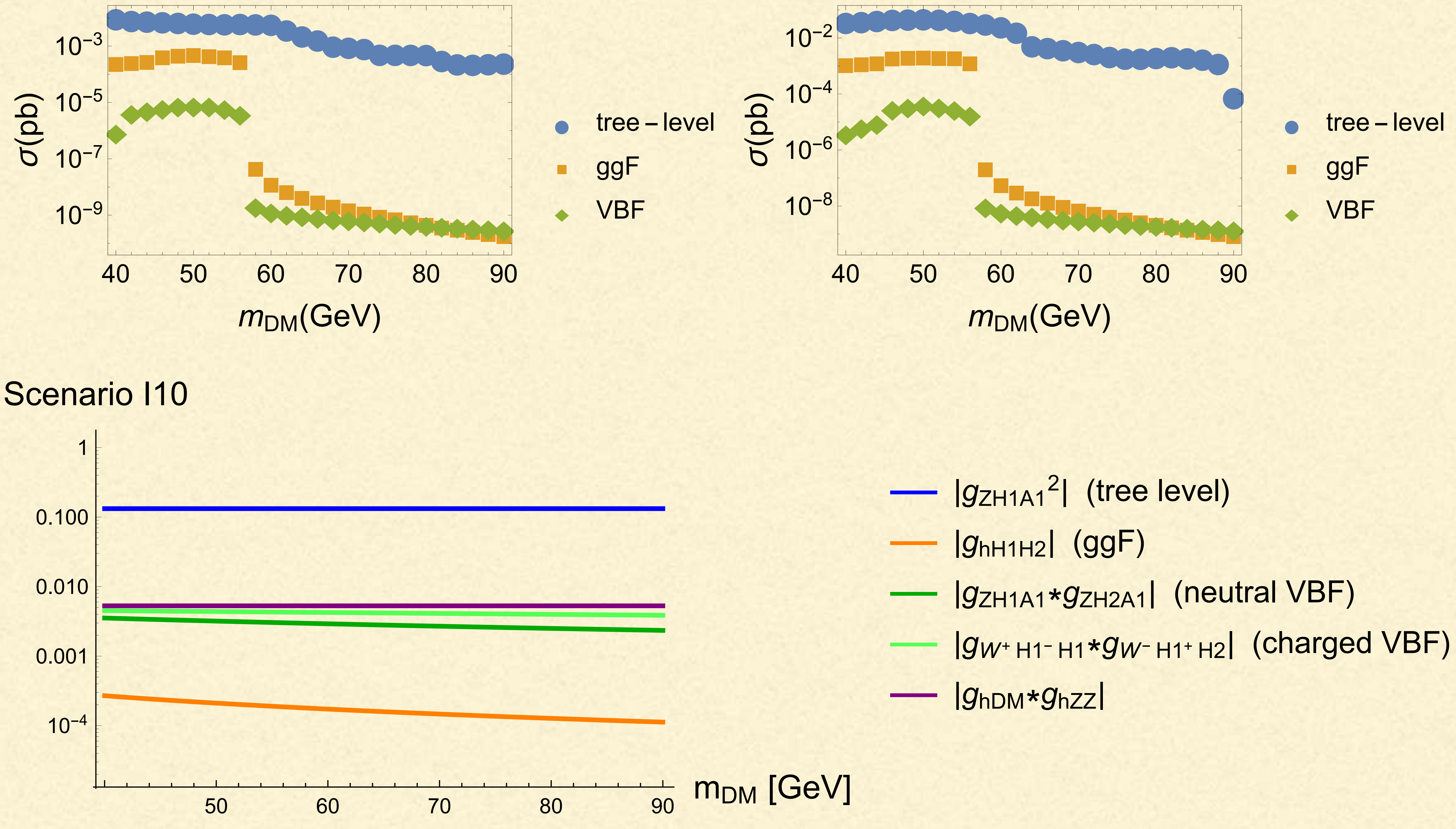

Scenario I10. The plots on the top show the cross sections of the tree-level, ggF and VBF processes with leptonic (left) and hadronic (right) final states. At the bottom we show the dominant couplings, where the Higgs-DM coupling is shown.

Benchmark	m_{H_1}	m_{H_2}	m_{A_1}	m_{A_2}	$m_{H_1^\pm}$	$m_{H_2^\pm}$	n	θ_h	$\sigma_{2\mu}$	$\sigma_{4\mu}$
BP1	50	55	95	104	116	127	0.83	0.105	0.02224	6.923
BP2	50	60	94	112	115	137	0.70	0.103	0.06	4.0

Definition of BPs with the masses shown in GeV. The last two columns show the cross sections for processes $\sigma_{2\mu} \equiv \sigma(pp \to H_2H_2 \to H_1H_1\ \mu^+\mu^-)$ and $\sigma_{4\mu} \equiv \sigma(pp \to H_2H_2 \to H_1H_1\ 2\mu^+\ 2\mu^-)$ in fb.

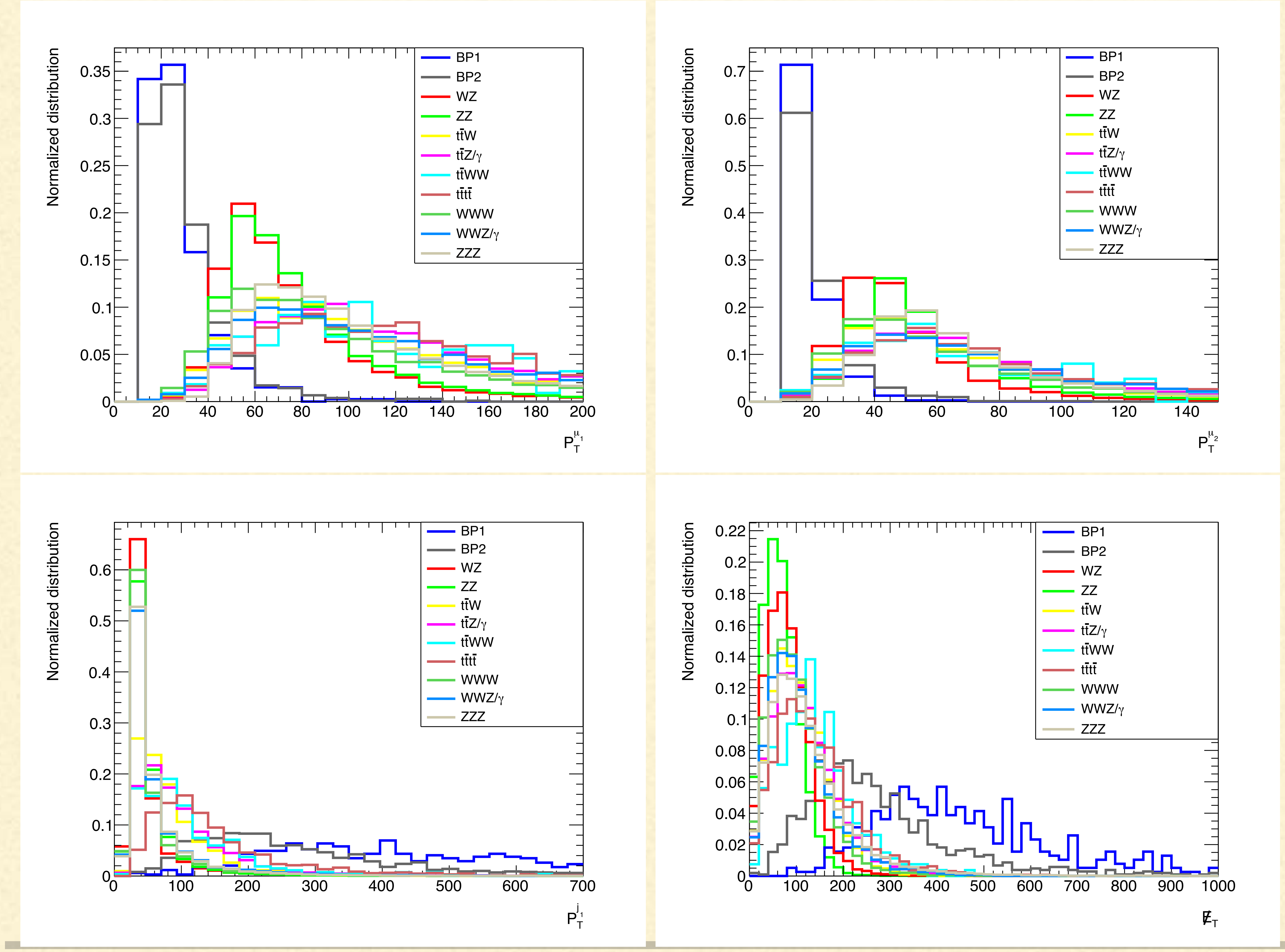

$$\mathcal{S} = \sqrt{2\left[(S+B)\,\log\left(1+\frac{S}{B}\right) - S\right]}.$$

	$\mathcal{S}$ (Pre-selection)	$\mathcal{S}$ (cut-A)
BP1	0.05 σ	3.35 σ
BP2	0.17 σ	10.15 σ

arXiv:2310.06593: A. Dey, V. Keus, S. Moretti, C. Shepherd-Themistocleous

I(2+1)HDM symmetric under $Z_2 \times Z'_2$,

$$
\begin{aligned}
V &= V_0 + V_{Z_2\times Z'_2}, \\
V_0 &= -\mu_1^2(\phi_1^\dagger\phi_1) - \mu_2^2(\phi_2^\dagger\phi_2) - \mu_3^2(\phi_3^\dagger\phi_3) + \lambda_{11}(\phi_1^\dagger\phi_1)^2 + \lambda_{22}(\phi_2^\dagger\phi_2)^2 + \lambda_{33}(\phi_3^\dagger\phi_3)^2 \\
&\quad +\lambda_{12}(\phi_1^\dagger\phi_1)(\phi_2^\dagger\phi_2) + \lambda_{23}(\phi_2^\dagger\phi_2)(\phi_3^\dagger\phi_3) + \lambda_{31}(\phi_3^\dagger\phi_3)(\phi_1^\dagger\phi_1) \\
&\quad +\lambda'_{12}(\phi_1^\dagger\phi_2)(\phi_2^\dagger\phi_1) + \lambda'_{23}(\phi_2^\dagger\phi_3)(\phi_3^\dagger\phi_2) + \lambda'_{31}(\phi_3^\dagger\phi_1)(\phi_1^\dagger\phi_3), \\
V_{Z_2\times Z'_2} &= \lambda_1(\phi_1^\dagger\phi_2)^2 + \lambda_2(\phi_2^\dagger\phi_3)^2 + \lambda_3(\phi_3^\dagger\phi_1)^2 + \text{h.c.},
\end{aligned}
$$

$$
g_{Z_2} = \text{diag}(-1,1,1)\,, \qquad g_{Z'_2} = \text{diag}(1,-1,1)\,.
$$

$$
\phi_1 = \begin{pmatrix} H_1^+ \\ \frac{H_1+iA_1}{\sqrt{2}} \end{pmatrix}, \quad \phi_2 = \begin{pmatrix} H_2^+ \\ \frac{H_2+iA_2}{\sqrt{2}} \end{pmatrix}, \quad \phi_3 = \begin{pmatrix} H_3^+ \\ \frac{v+h+iA_3^0}{\sqrt{2}} \end{pmatrix},
$$

$$
m_h^2 = 2\mu_3^2 = 2v^2\lambda_{33}
$$

THEORETICAL AND EXPERIMENTAL CONSTRAINTS

2012.11621 [hep-ph] and 2202.10514 [hep-ph]

- EW precision Test (EWPT)
- Collider data LEP and LHC: Higgs total decay width, Higgs invisible decays, on-shell decays from Z, W.
- The DM relic density.
- DD and ID detection.
- Being (H_1, H_2) or (H_1, A_2) DM candidates: work in progress.

BP	m_{H_1}	m_{A_1}	$m_{H_1^\pm}$	m_{H_2}	m_{A_2}	$m_{H_2^\pm}$	Λ_1	$g_{hH_1H_1}$	$g_{hH_2H_2}$	$g_{hA_1A_1}$	$g_{hA_2A_2}$	$\Omega_{H_1}h^2$	$\Omega_{H_2}h^2$
BP1	80	120.4	130	80	110.6	130	0.082	0.1916	0.1832	0.2492	0.2197	0.0032	0.0033

BP	m_{H_1}	m_{A_1}	$m_{H_1^\pm}$	m_{H_2}	m_{A_2}	$m_{H_2^\pm}$	Λ_1	$g_{hH_1H_1}$	$g_{hH_2H_2}$	$g_{hA_1A_1}$	$g_{hA_2A_2}$	$\Omega_{H_1}h^2$	$\Omega_{H_2}h^2$
BP2	80	120.4	130	110.6	80	130	0.0343	0.1916	0.0113	0.46	-0.1815	0.004	0.005

Table 1: The parameter values for BP1 and BP2. In both cases, we have set $\lambda_{11} = 0.11$, $\lambda_{22} = 0.12$, $\lambda_{12} = 0.121$, $\lambda'_{12} = 0.13$, the SM Higgs mass $m_h = 125$ GeV and $v = 246$ GeV, are in agreement with all astrophysical and collider constraints. For the BP1, the cross section is $\sigma(e^+e^- \to H_1H_1/H_2H_2 + \ell\bar{\ell}) = 5.9$ fb and for the BP2, it is $\sigma(e^+e^- \to H_1H_1/A_2A_2 + \ell\bar{\ell}) = 6.1$ fb for 500 GeV centre of mass energy. For BP1, the cross section is $\sigma(e^+e^- \to H_1H_1/H_2H_2 + \ell\bar{\ell}) = 2.1$ fb and for the BP2, it is $\sigma(e^+e^- \to H_1H_1/A_2A_2 + \ell\bar{\ell}) = 1.7$ fb for 1 TeV centre of mass energy.

$e^+e^- \to DMDM\ell^+\ell^-$ (for ILC machine)

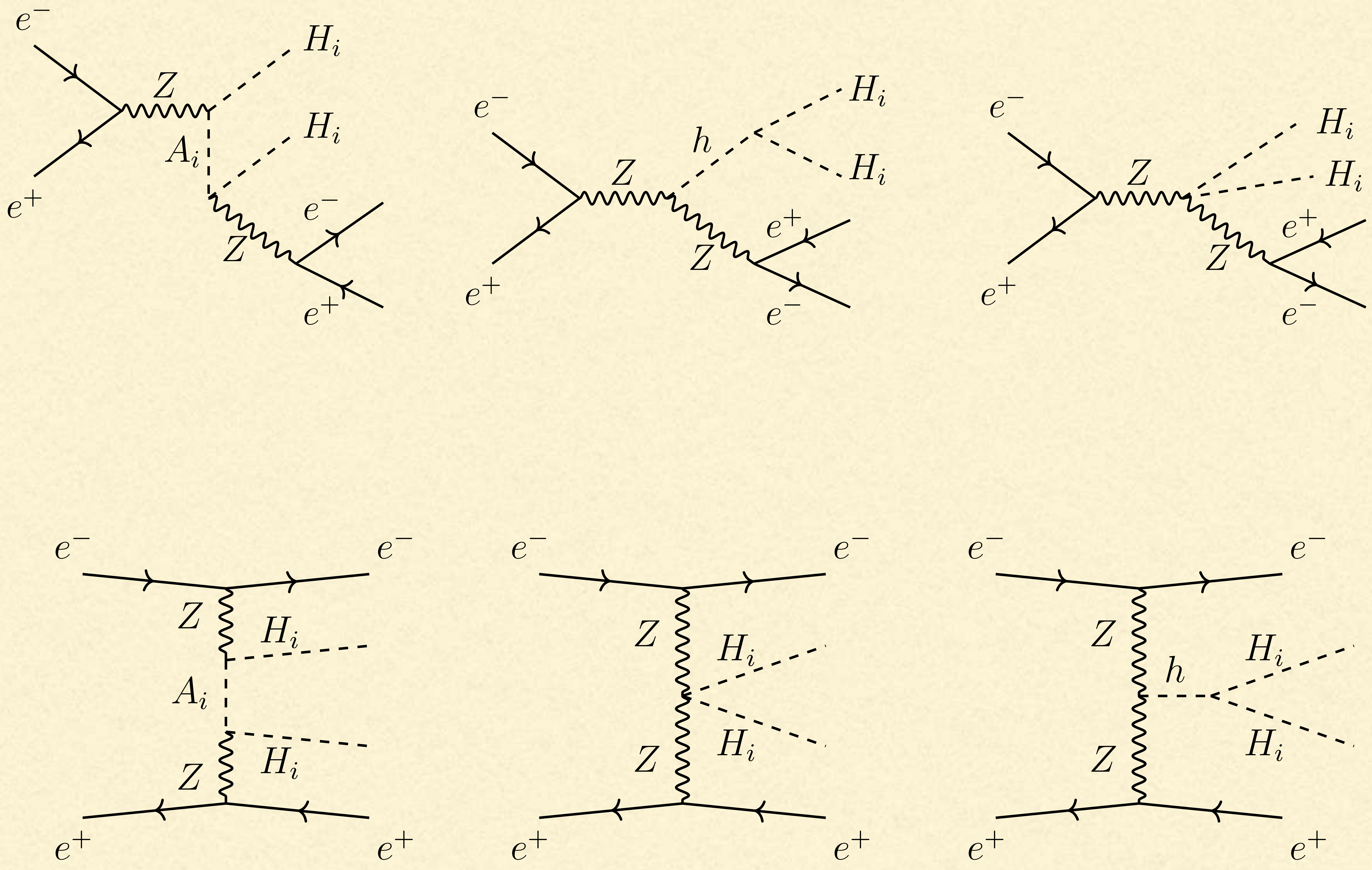

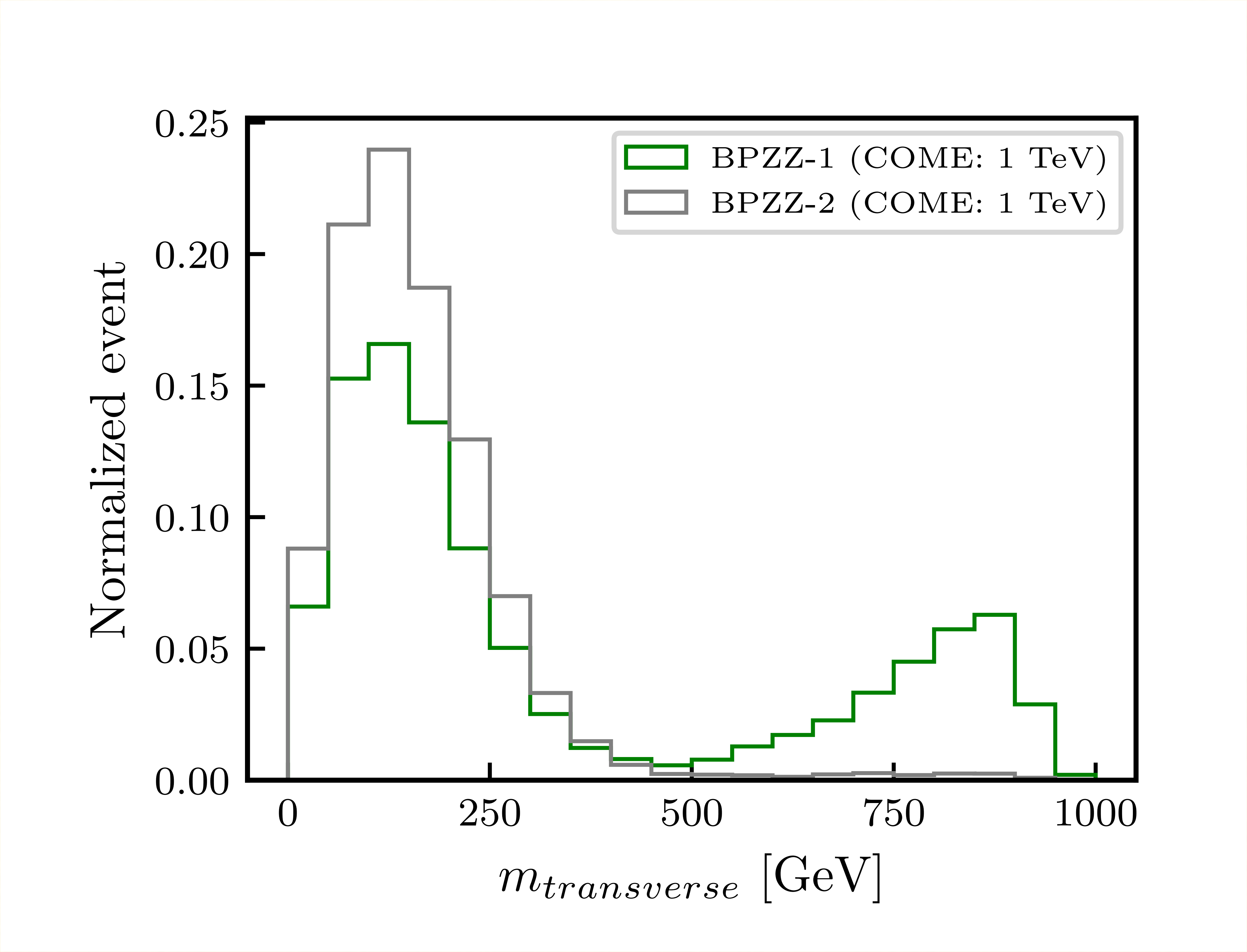

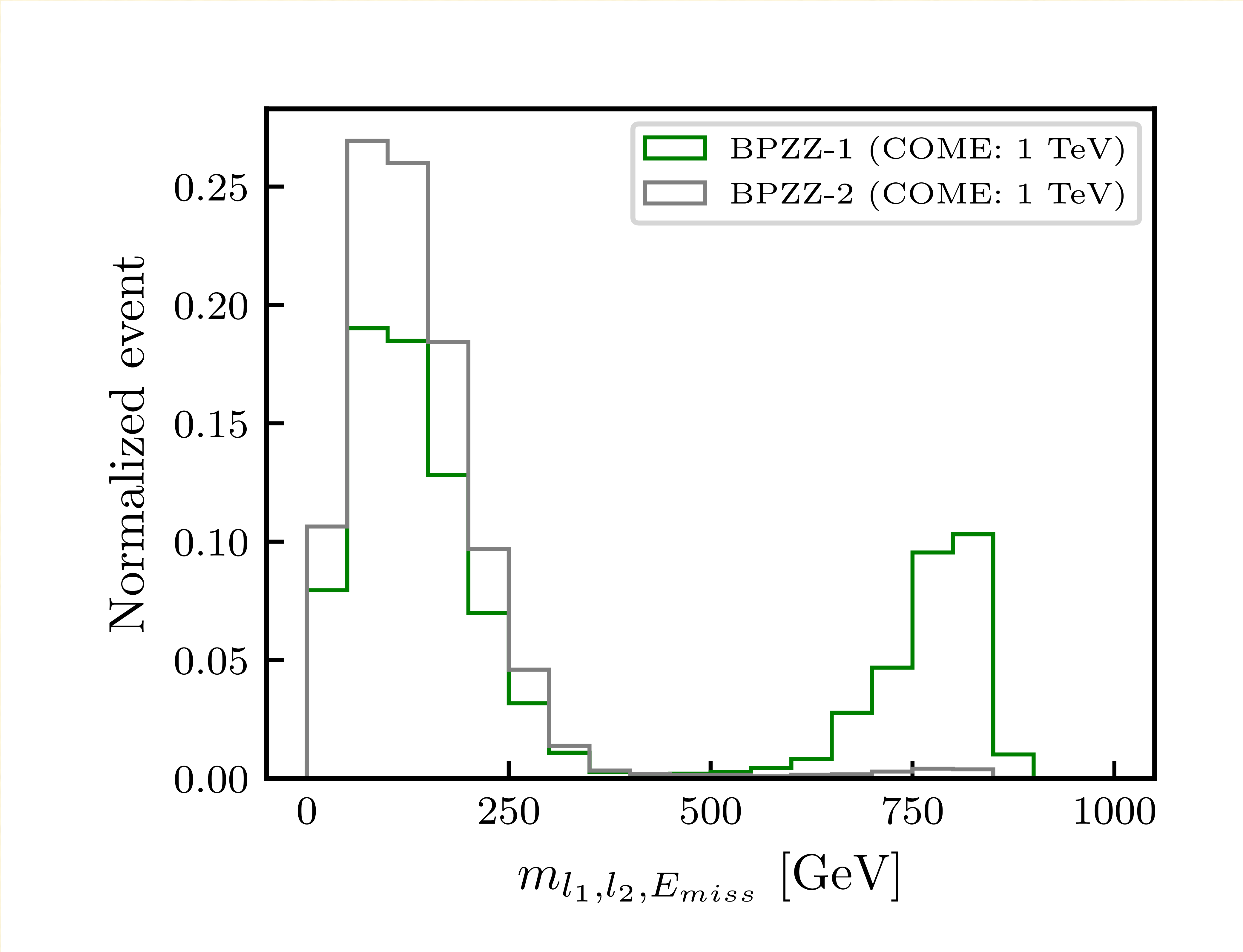

Normalized distribution of the transverse mass of two lepton and missing energy final state, at 1 TeV ILC with e− and e+ are 80% and 30% polarized, respectively, for BP1 and BP2 after detector simulation.

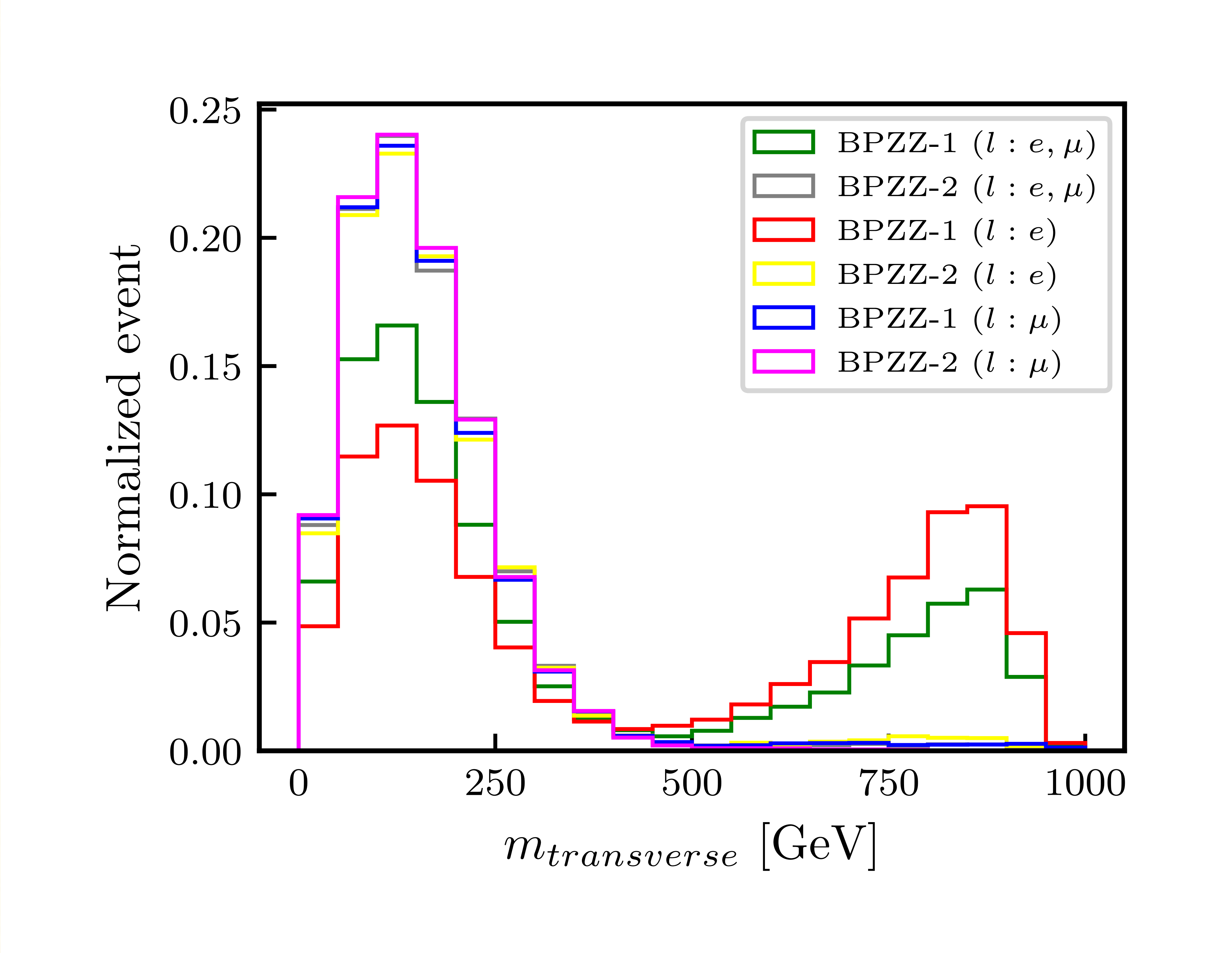

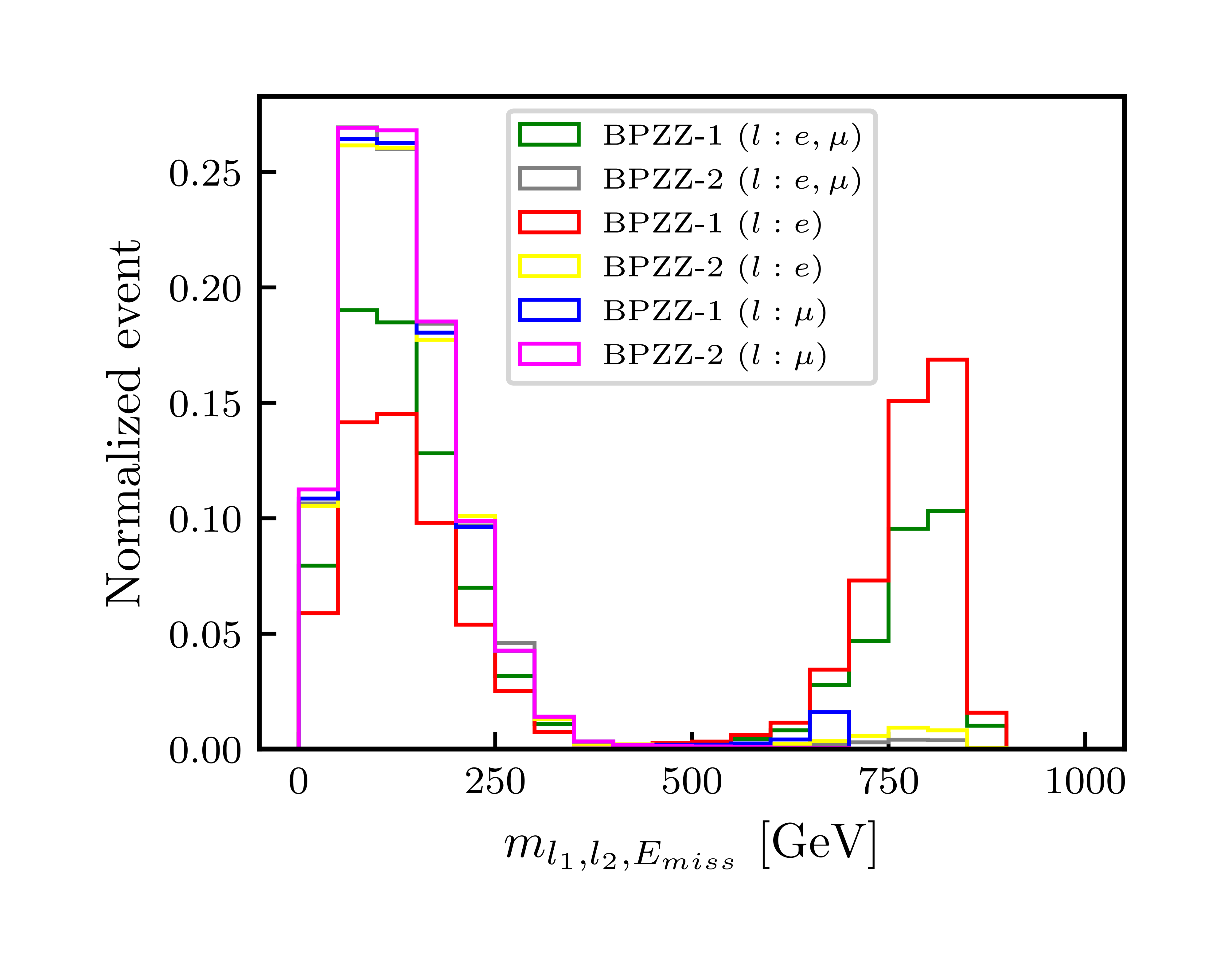

Normalized distribution of the transverse mass of two lepton and missing energy final state, at 1 TeV ILC with e− and e+ are 80% and 30% polarized, respectively, for BP1 and BP2 after detector simulation.

I(2+1)HDM symmetric under Z_3 (1907.12470 [hep-ph])

$$V_0 = -\mu_1^2(\phi_1^\dagger\phi_1) - \mu_2^2(\phi_2^\dagger\phi_2) - \mu_3^2(\phi_3^\dagger\phi_3) \\ +\lambda_{11}(\phi_1^\dagger\phi_1)^2 + \lambda_{22}(\phi_2^\dagger\phi_2)^2 + \lambda_{33}(\phi_3^\dagger\phi_3)^2 \\ +\lambda_{12}(\phi_1^\dagger\phi_1)(\phi_2^\dagger\phi_2) + \lambda_{23}(\phi_2^\dagger\phi_2)(\phi_3^\dagger\phi_3) + \lambda_{31}(\phi_3^\dagger\phi_3)(\phi_1^\dagger\phi_1) \\ +\lambda'_{12}(\phi_1^\dagger\phi_2)(\phi_2^\dagger\phi_1) + \lambda'_{23}(\phi_2^\dagger\phi_3)(\phi_3^\dagger\phi_2) + \lambda'_{31}(\phi_3^\dagger\phi_1)(\phi_1^\dagger\phi_3),$$

$$\phi_1 \to \omega\phi_1 \ , \quad \phi_2 \to \omega^2\phi_2 \ , \quad \phi_3 \to \phi_3 \ ,$$

$$\omega = e^{2\pi i/3}. \qquad g_{Z_3} = \text{diag}\left(\omega, \omega^2, 1\right).$$

$$V_{Z_3} = \lambda_1(\phi_2^\dagger\phi_1)(\phi_3^\dagger\phi_1) + \lambda_2(\phi_1^\dagger\phi_2)(\phi_3^\dagger\phi_2) + \lambda_3(\phi_1^\dagger\phi_3)(\phi_2^\dagger\phi_3) + h.c.$$

$$m_{H_1}^2 = m_{A_1}^2 = \cos^2\theta_h(-\mu_1^2 + \Lambda_1) + \sin^2\theta_h(-\mu_2^2 + \Lambda_2) + \sin\theta_h\cos\theta_h\lambda_3 v^2$$
$$m_{H_2}^2 = m_{A_2}^2 = \sin^2\theta_h(-\mu_1^2 + \Lambda_1) + \cos^2\theta_h(-\mu_2^2 + \Lambda_2) - \sin\theta_h\cos\theta_h\lambda_3 v^2$$

Coulb be posible to have two DM candidates H_1, A_1: we called hermaphrodite DM scenario

$e^+e^- \rightarrow DMDM\ell^+\ell^-$ (for ILC machine)

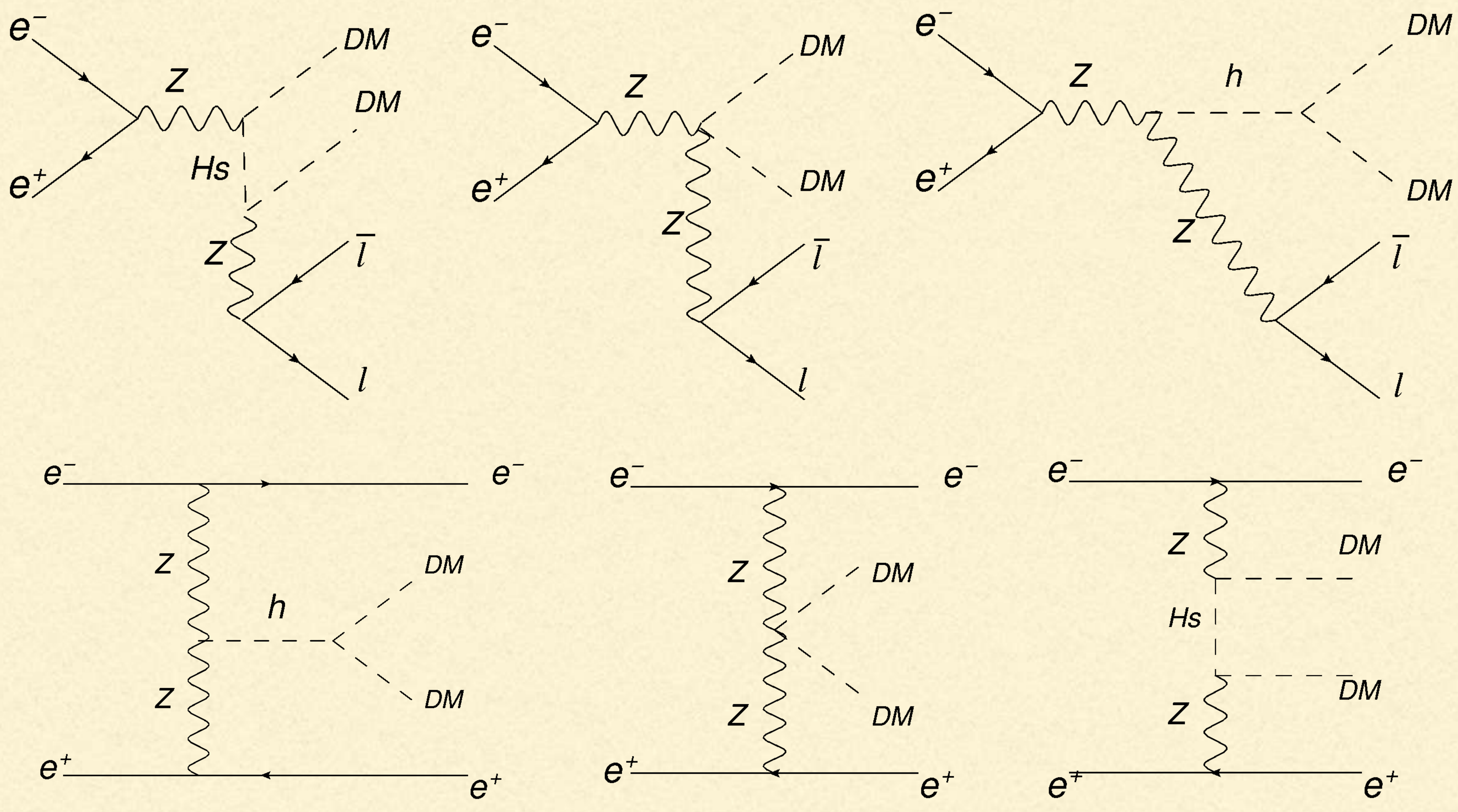

Feynman diagrams for the processes $e^+e^- \rightarrow 2l + 2DM$, where $l = e^-(\mu^-)$ and $\bar{l} = e^+(\mu^+)$, Hs = A2(H2) and DM = H1(A1).

We can compare with the cases of $Z_2 \times Z_2'$ shown previously

Signals in electron-proton colliders like LHeC, FCC-he:

Signals in electron-proton colliders like LHeC, FCC-he: $e^- p \to DMDMj\ell^-$ or $e^- p \to DMDMj\nu$ or considering cascades of heavier scalar inserts having the final signatures: $\not{E}_T\, j$, $\not{E}_T \ell j$, $\not{E}_T 2\ell j$, $\not{E}_T 3\ell j$ (work in progress)

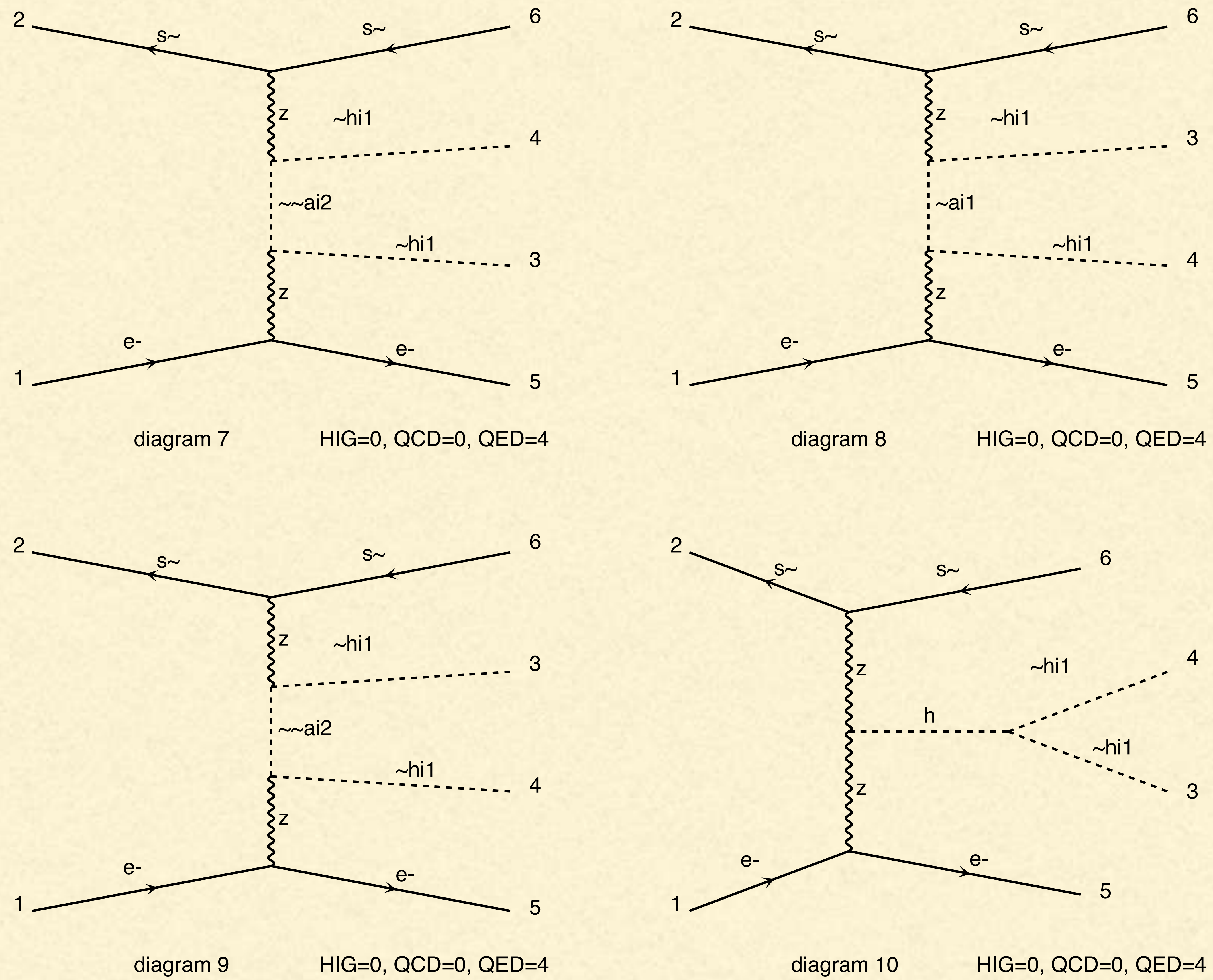

CONCLUSIONS

- We study 3HDM (in version I(2+1)HDM) symmetric under Z_2, $Z_2 \times Z_2'$ and Z_3, we analyze interesting signals of DM that could be tested in the colliders: LHC, ILC and LHeC.
- In the I(2+1)HDM symmetric under Z_2, we analyze the cascade decay:
  - $h \to H_1 H_2 \to H_1 H_1 f\bar{f}$ as a smoking-gun signal of 3HDM,
  - $H_2 \to H_1 \gamma^* \to H_1 f\bar{f}$ is induced at one-loop level.
- In the I(2+1)HDM symmetric under $Z_2 \times Z_2'$ (with two DM candidates): we study $e^+e^- \to DMDM\ell^+\ell^-$ (for ILC machine) in two cases:
  - The two DM candidates have the same CP (H_1, H_2) and opposite CP in another (H_1, A_2)
  - The distributions of observables for this collider can distinguish clearly both cases
- Outlooks:
- Special case of I(2+1)HDM symmetric under Z_3 (we called hermaphrodite DM scenario): two DM candidates (H_1, A_1) and for ILC machine could be tested and distinguished with the case $Z_2 \times Z_2'$.
- Signals in electron-proton colliders like LHeC, FCC-he: $e^-p \to DMDMj\ell^-$ or $e^-p \to DMDMj\nu$ or considering cascades of heavier scalar inserts having the final signatures: $\not{E}_T\, j$, $\not{E}_T \ell j$, $\not{E}_T 2\ell j$, $\not{E}_T 3\ell j$

Variable	Description
$P_{T\ell_1}$	Transverse momentum of leading lepton (the lepton that carries highest momentum)
$P_{T\ell_2}$	Transverse momentum of sub-leading lepton (the lepton carries second highest momentum)
$\not{E}_T$	Missing transverse momentum
E_{miss}	Missing energy
H_T	Scalar sum of transverse momentum of two leading leptons and missing energy
$m_{transverse}$	Transverse mass of final state including two lepton and missing energy
m_{ℓ_1,ℓ_2}	Invariant mass of two leading leptons
$m_{\ell_1,\ell_2,E_{miss}}$	Invariant mass of two leading leptons and missing energy system
$\Delta\eta_{\ell_1,\ell_2}$	Difference of pseudo-rapidity between two leading leptons with highest momentum
$\Delta\eta_{\ell_1,E_{miss}}$	Difference of pseudo-rapidity between leading lepton with highest momentum and missing energy direction
$\Delta R_{\ell_1,\ell_2}$	Radial distance between two leading leptons with highest momentum
$\Delta R_{\ell_1,E_{miss}}$	Radial distance between two leading lepton with highest momentum and missing energy direction
$\Delta\phi_{\ell_1,\ell_2}$	Difference of azimuthal angle between two leading leptons with highest momentum
$\Delta\phi_{\ell_1,\not{E}_T}$	Difference of azimuthal angle between leading lepton and missing energy
$\Delta\phi_{l^-,\not{E}_T}$	Difference of azimuthal angle between negatively charged lepton and missing energy
P_θ	Energy imbalance between missing energy and two leading lepton system